SF2A 2023
M. N'Diaye, A. Siebert, N. Lagarde, O. Venot, K. Baillié, M. Béthermin, E. Lagadec, J. Malzac, J. Richard (eds)

NEW FEATURES OF PHASE SPIRAL FROM GAIA DR3

C. Li[1], A. Siebert[1], G. Monari[1], B. Famaey[1] and S. Rozier[2]

Abstract. Disc stars from the Gaia DR3 RVS catalogue are selected to explore the phase spiral in the Galaxy. The data reveal a two-armed phase spiral pattern in the local $z - v_z$ plane inside the solar radius, which appears clearly when colour-coded by $\langle v_R \rangle(z, v_z)$: this is characteristic of a breathing mode that can in principle be produced by in-plane non-axisymmetric perturbations. The phase spiral pattern becomes single armed outside the solar radius. When a realistic analytic model with a steadily rotating bar and 2-armed spiral arms as perturbation is used to perform particle test integrations, no phase-spiral is perceptible in the (z, v_z) plane. Finally, we show as a proof of concept how a toy model of a time-varying non-axisymmetric in-plane perturbation with varying pattern speed can produce a strong two-armed phase-spiral. We conclude a time-varying strong internal perturbation together with an external vertical perturbation could perhaps explain the transition between the two-armed and one-armed phase-spirals around the Solar radius.

Keywords: Galaxy: kinematics and dynamics – Galaxy: evolution – Galaxy: structure – Galaxy: disc

1 Introduction

The phase spiral structure in the vertical position and velocity (z, v_z) plane of the Milky Way is one of the most important discoveries since the launch of the Gaia mission (Gaia Collaboration et al. 2016). This feature was first revealed in the solar vicinity with a population of stars sharing similar Galacto-centric radii and azimuthal angles (Antoja et al. 2018). Usually, the phase spiral is supposed to be generated by an external perturber such as a dwarf galaxy merging with the Milky Way. Binney & Schönrich (2018), for instance, developed a toy model based on the impulse approximation to show that the perturbation imposed by an intruder (such as a dwarf galaxy or some dark matter subhalo) can cause a prominent phase spiral in $\langle v_\phi \rangle(z, v_z)$. A concurrent explanation of the phase spiral associates it with internal mechanisms within the disc. In particular, Khoperskov et al. (2019) used an N-body simulation of an isolated Milky Way-type galaxy to show that the vertical oscillations driven by bar buckling can generate phase spirals in the solar neighbourhood.

Recently, using Gaia DR3 observations of inner disk stars, Hunt et al. (2022) spotted a two-armed spiral feature in $\rho(z, v_z)$ when stars are binned by guiding radius R_g and θ_ϕ, the conjugate angle of the action J_ϕ. Interestingly, they also found such a two-armed phase spiral in an isolated simulation. Recently, the framework of the shearing box approximation was adopted by Widrow (2023) to investigate the response of a disc to an impulsive excitation in the presence of self-gravity of the disc and swing amplification.

In light of the recently discovered two-armed phase spiral inside the solar radius, which can be produced by internal plane-symmetric perturbations, this paper aims at analysing what kind of phase spiral could potentially be produced by the bar and spiral arms of the Galaxy. We then compare the data, for the time being at the *qualitative* level, to test-particle simulations in a galactic potential with different bar and spiral arms perturbations added on top of a self-consistent background axisymmetric model.

2 Phase space spirals with Gaia DR3

Figure 1 shows the density plot of the sample stars in the $z - v_z$ phase space binned by the value of their angular momentum J_ϕ. The resulting density $\rho(z, v_z)$ is then smoothed by convolution with a Gaussian filter of width

[1] Université de Strasbourg, CNRS, Observatoire astronomique de Strasbourg (ObAS), UMR 7550, 67000 Strasbourg, France
[2] School of Mathematics, University of Edinburgh, Kings Buildings, Edinburgh, EH9 3FD, UK

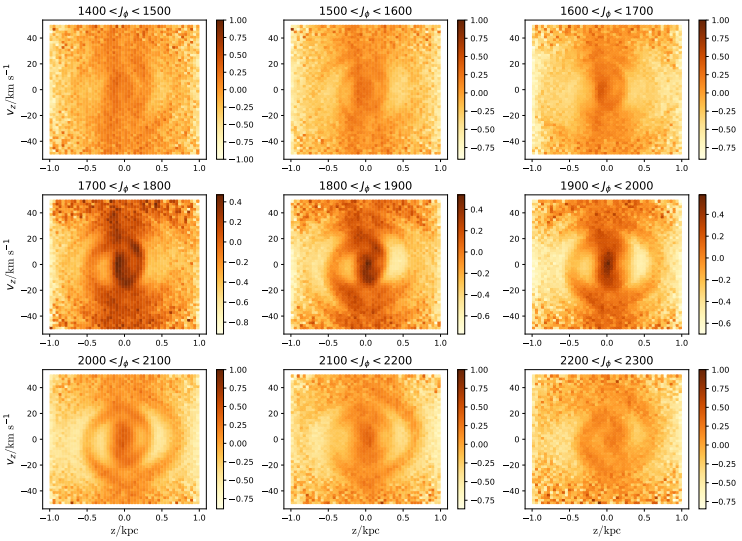

Fig. 1. The phase space density plot for our selected Gaia RVS sample data. The plotted quantity is the relative overdensity w.r.t. an average local density, following a procedure introduced in the text in detail. Only one armed phase spirals are seen in different J_ϕ intervals.

$4\,\Delta$pix, yielding the smoothed density $\bar{\rho}(z, v_z)$. We then plot the overdensity $\hat{\rho} = \rho(z, v_z)/\bar{\rho}(z, v_z) - 1$. Different panels correspond to different azimuthal action bins, which is an increasing function of the guiding radius R_g: $J_\phi = R_\mathrm{g} \times v_\mathrm{c}(R_\mathrm{g})$.

A single spiral pattern appears clearly in most panels, although this is not clear for the three innermost (lowest angular momenta) bins due to the large scatters of the data points in these bins. This one-armed phase spiral, as discussed thoroughly in the literature, could be related to a bending mode in the local and outer Galaxy, which could be triggered by the impact of the Sagittarius dwarf galaxy (e.g., Binney & Schönrich 2018; Bland-Hawthorn & Tepper-García 2021).

Several previous works have shown that the phase spiral can sometimes appear more clearly, and with different characteristics, either in the $\langle v_R \rangle(z, v_z)$ and $\langle v_\phi \rangle(z, v_z)$ maps (e.g. Antoja et al. 2018; Binney & Schönrich 2018; Bland-Hawthorn & Tepper-García 2021). Figure 2 therefore displays the mean Galactocentric radial velocity maps $\langle v_R \rangle(z, v_z)$ in different J_ϕ bins. The results are particularly interesting in the inner Galaxy. The first four panels, with $1400\,\mathrm{km\ s^{-1}kpc} < J_\phi < 1800\,\mathrm{km\ s^{-1}kpc}$, indeed show clear *two-armed* spiral patterns. When $J_\phi > 1800$ km s^{-1} kpc (next five panels), only one-armed spiral features can be seen in the plots, as in the density maps of Fig. 1. The two-armed phase-spiral pattern corresponds to a breathing wave (e.g., Widrow 2023) and is a strong hint for another perturbation mechanism than the perturbation causing the one-armed spiral in the outer disc (Hunt et al. 2022).

3 Modelling predictions under perturbations

3.1 Results for steadily rotating perturbations

Figure 3 shows the phase space maps of $\rho(z, v_z)$ (top row) and $\langle v_R \rangle(z, v_z)$ (bottom row) for different positions along the disc at $T = 1.5$ Gyr for a steadily rotating bar model. Unlike the observational data, the density plot $\rho(z, v_z)$ shows no spiral arm features among different azimuthal action intervals. Furthermore, the $\langle v_R \rangle(z, v_z)$ plots do not show any sign of phase spirals either. The distribution of $\langle v_R \rangle(z, v_z)$ is smooth within the central region of the $z - v_z$ plane and gets progressively noisy outwards. We did test the pseudo stars phase space properties for other snapshots at various time steps in the simulation: there are no phase spiral structures either in the (z, v_z) plane, whether it is in density or colour-coded by velocities.

3.2 Time-varying strong bar toy-model

To demonstrate that such two-armed phase spirals can *in principle* be produced by plane-symmetric perturbations, we now explore a toy-model of a strong bar with a time-varying pattern speed. We consider a bar with a large initial pattern speed and let the pattern speed decrease with time. The bar model we use in this toy-simulation is from Sormani et al. (2022). The initial pattern speed is $\Omega_\mathrm{b} = -88\,\mathrm{km\ s^{-1}\,kpc^{-1}}$ at $T = 0$ Gyr.

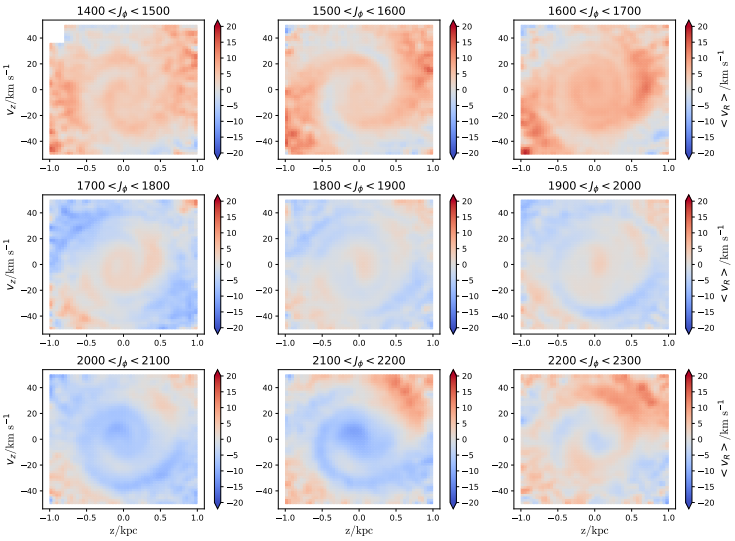

Fig. 2. The phase space plot colour-coded by $\langle v_R \rangle$ for our selected Gaia RVS sample data. Two armed phase spirals are clearly seen inside the solar radius when $J_\phi < 1800\,\mathrm{km\ s^{-1}kpc}$. The phase spiral pattern becomes single armed when $J_\phi > 1800\,\mathrm{km\ s^{-1}kpc}$.

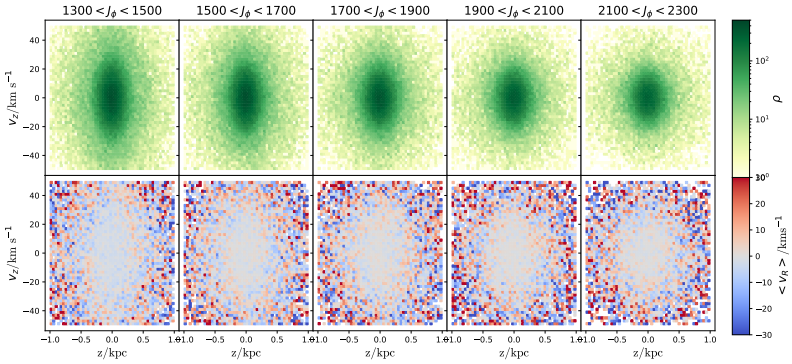

Fig. 3. Maps of $\rho(z, v_z)$ (top) and $\langle v_R \rangle(z, v_z)$ (bottom) for the model including a bar and spiral arms with constant pattern speeds, at $T = 1.5$ Gyr. Both the density $\rho(z, v_z)$ and $\langle v_R \rangle(z, v_z)$ show no spiral arm features.

Then it immediately starts to decrease and reach $\Omega_\mathrm{b} = -35\,\mathrm{km\ s^{-1}\,kpc^{-1}}$ at $T = 6$ Gyr. Meanwhile, the mass and radial profile of the bar are set to be multiplied by factors 2.5 and 1.5 respectively, which roughly simulates the growth of the bar. We then integrate test particle orbits for 8 Gyr. This extreme model is not meant to represent the real Milky Way in any way, but is rather meant, as a proof of concept, to strongly disturb the disk in a plane-symmetric way whilst not letting the pseudo stars settling within the potential of the perturber whose pattern speed constantly varies with time.

Figure 4 then shows the $z - v_z$ phase space density of the pseudo stars at $T = 3.0$ Gyr in the upper panels and $T = 3.5$ Gyr in the lower panels. It shows clear 2-armed spiral features in the first two panels at $T = 3.0$ Gyr. We also tested constant pattern speed bar models with the same spiral arm potential as in this model, and only this one produced the bisymmetric phase spiral, which is strong evidence that a bar with varying pattern speed is likely the culprit generating perturbations to the disc stars that lead to a 2-armed phase space spiral structure. The same pattern can also be seen in $\langle v_R \rangle(z, v_z)$ at $T = 3.0$ Gyr in the first panel.

4 Conclusions

In this work, we investigated the Gaia phase spiral structure based on observational data from Gaia DR3. We see a clear two-armed phase spiral structure in the inner disc in the $\langle v_R \rangle(z, v_z)$ map. On the contrary, only a one-armed phase spiral structure is clearly seen in the $\rho(z, v_z)$ plots. In order to analyse the possible origin of the two-armed phase spiral structure, we used test particle simulations to investigate how such perturbations affect the vertical phase space structure of the Galactic disc.

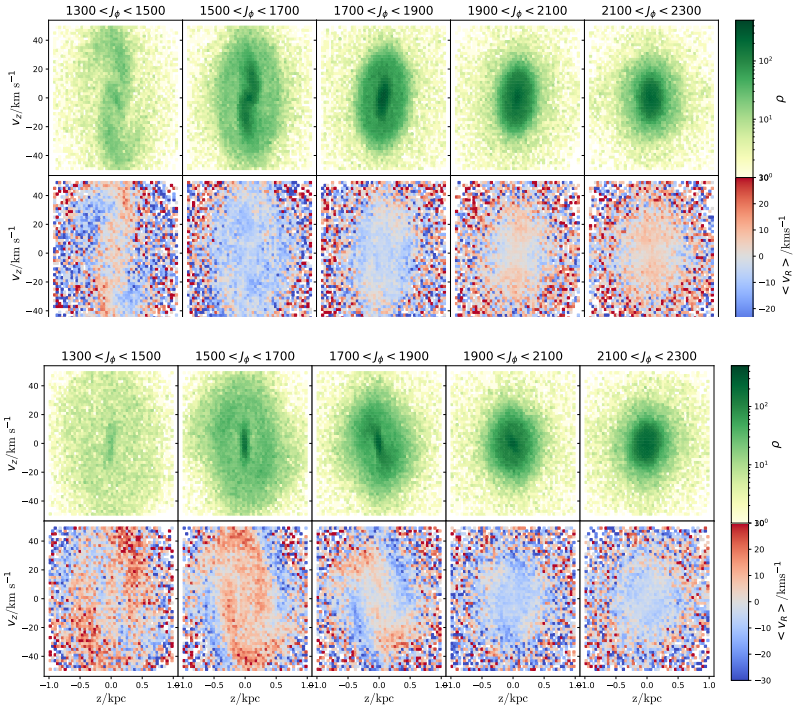

Fig. 4. Maps of $\rho(z, v_z)$ and $\langle v_R \rangle(z, v_z)$ for test particles in the model with decreasing bar pattern speed, at $T = 3.0$ Gyr (upper grid) and $T = 3.5$ Gyr (lower grid). In each grid, the top row shows the density $\rho(z, v_z)$ and the bottom row $\langle v_R \rangle(z, v_z)$. The density plot $\rho(z, v_z)$ shows clear 2-armed spiral features in the first two panels at $T = 3.0$ Gyr. The 2-armed spiral feature can also be seen in the first panel of $\langle v_R \rangle(z, v_z)$. At $T = 3.5$ Gyr, the 2-armed spiral feature in $\rho(z, v_z)$ is eliminated but still clear in $\langle v_R \rangle(z, v_z)$.

First, we showed that a realistic bar and spiral arm pattern with constant amplitude and pattern speed generates, as expected, non-zero mean v_R values across the disc, while the mean v_z remains null because the perturbations are plane-symmetric. The subtraction of the mean v_z values in the North and South hemisphere above and below the Galactic plane demonstrate, as expected too, that the Galaxy undergoes a breathing mode, which is particularly visible in the inner Galaxy. However, this breathing mode only translates itself in an inclination of the $z - v_z$ ellipsoid but does not show any sign of a two-armed phase spiral.

Therefore, we also tested the ability to disturb the disc with a stronger bar with varying pattern speed, not allowing the pseudo stars to settle in the potential of the perturber due to a constantly evolving potential. In this toy-model, we find that the phase space density $\rho(z, v_z)$ does show clear 2-armed spiral features, which is strong evidence that a bar with a decreasing pattern speed is able to produce a 2-armed phase spiral. This result suggests that the pattern speed of the bar might not be constant over time in the real Galaxy. We note that it takes a long time to produce these two-armed phase spirals and that the phase spiral features appear from inside-out, probably related to the growth of the bar.

References

Antoja, T., Helmi, A., Romero-Gómez, M., et al. 2018, Nature, 561, 360
Binney, J. & Schönrich, R. 2018, MNRAS, 481, 1501
Bland-Hawthorn, J. & Tepper-García, T. 2021, MNRAS, 504, 3168
Gaia Collaboration, Prusti, T., de Bruijne, J. H. J., et al. 2016, A&A, 595, A1
Hunt, J. A. S., Price-Whelan, A. M., Johnston, K. V., & Darragh-Ford, E. 2022, MNRAS, 516, L7
Khoperskov, S., Di Matteo, P., Gerhard, O., et al. 2019, A&A, 622, L6
Sormani, M. C., Gerhard, O., Portail, M., Vasiliev, E., & Clarke, J. 2022, MNRAS, 514, L1
Widrow, L. M. 2023, MNRAS, 522, 477